Article

An NIR Neodymium-Tag for Quantifying Targeted Biomarker and Counting Its Host Circulating Tumor Cells

Chunlan Liu, Shu Lu, Limin Yang, Peijie Chen, Peiming Bai, and Qiuquan Wang

Anal. Chem., **Just Accepted Manuscript** • DOI: 10.1021/acs.analchem.7b02016 • Publication Date (Web): 26 Jul 2017

An NIR Neodymium-Tag for Quantifying Targeted Biomarker and Counting Its Host Circulating Tumor Cells

Chunlan Liu,[†] Shu Lu,[‡] Limin Yang,[†] Peijie Chen,[‡] Peiming Bai,[*,‡] Qiuquan Wang[*,†,§]

[†]Department of Chemistry & the MOE Key Laboratory of Spectrochemical Analysis and Instrumentation, College of Chemistry and Chemical Engineering, Xiamen University, Xiamen 361005, China
[‡]Department of Urology, Zhongshan Hospital, Xiamen University, Xiamen 361004, China
[§]State Key Lab of Marine Environmental Science, Xiamen University, Xiamen 361005, China
Fax no.: +86 592 2187400; e-mail: qqwang@xmu.edu.cn; baipeiming@xmu.edu.cn

ABSTRACT: Quantitative information of targeted analyte in a complex biological system is the most basic premise for understanding its involved mechanisms, and thus precise diagnosis of a disease if it is a so-called biomarker. Here, we designed and synthesized a neodymium (Nd)-cored tag [1,4,7,10-tetraazacyclododecane-1,4,7-trisacetic acid (DOTA)-Nd complex together with a light-harvesting antenna aminofluorescein (AMF, $\lambda_{ex/em}$ = 494/520 nm), AMF-DOTA-Nd] with duplex signals, second near-infrared (NIR) window luminescence (λ_{em} = 1065 nm, 2.5 μs) and stable isotopic mass (^{142}Nd). AMF-DOTA-Nd covalently linked with an urea-based peptidomimetic targeting group, 2-[3-(1,3-dicarboxypropyl)-ureido]pentanedioic acid (DUPA)-8-Aoc-Phe-Phe-Cys (DUPA*aFFC*) (DUPA*aFFC*-AMF-DOTA-Nd), allowing us to detect and quantify prostate-specific membrane antigen (PSMA) and its splice variants (total PSMA, *t*PSMA), which was set as an example of targeted biomarkers in this study, using NIR and ICPMS with the LOD (3σ) of 0.3 ng/mL. When it was applied to the analysis of 80 blood samples from prostate cancer (PCa) and benign prostatic hyperplasia (BPH) patients as well as healthy volunteers, we found that 320 and 600 ng/mL *t*PSMA could be recommended as the threshold values to differentiate BPH from PCa and for the diagnosis of PCa. Moreover, PSMA-positive CTCs were counted using ICPMS being from 134 to 773 CTCs in the PCa blood samples of the Gleason score from 6 to 9 when the cell membrane-spanning *m*PSMA was tagged. Such a methodology developed could be expected to be applicable to other clinic-meaningful biomolecules and their host CTCs in liquid biopsy, when other specific targeting groups are modified to the NIR Nd-tag.

Today organic fluorophores, rather than the traditional radioactive isotopes, are more widely used for detecting and tracking biomolecules and cells owing to their spatial and temporal resolution and nonradioactive optical properties as well.[1-3] Even so, we know that they frequently encounter the drawbacks such as narrow stokes shift between excitation and emission wavelengths, unexpected photostability (such as photobleaching and quenching), in addition to the possible optical interferences of self-fluorescence and scattering from the extremely intricate biomatrix in the UV-visible region.[4,5] Fortunately, bioanalysis based on the luminescent lanthanides (Ln), which can be sensitized by energy transfer from the outfitted light-harvesting antenna, benefits from bigger 'stokes shift' to the spectral range of near-infrared (NIR) starting formally from first NIR window 650-950 nm through second NIR window 950-1400 nm and even extending up to 2500 nm.[6,7] The NIR luminescence can not only permeate into the body without intense absorbance and scattering by biological matrix, but also avoid the self-fluorescence background in the UV-visible region; and the long excited emitting lifetime features the time-resolved detection possible.[8,9] Such advantages do make Ln-centered probes being superior optical reporters compared to their organic analogues in bioanalysis, yet hard to be quantitative, only providing qualitative trends in signal intensity change since precise concentration of the reporter must be known and, symmetry of the ligand sphere of the coordinatively unsaturated Ln-complexes must be maintained.[10-12] These are difficult to know and control in a very complicated biosystem. A ratiometric measurement by modulating the peak ratio of respective emission profile has to be performed to solve this problem using, for example, the cocktails of $Tb^{3+}$and Eu^{3+} complexes because of their different optical but nearly identical physicochemical behavior in solution.[13,14]

On the other hand, the nonradioactive Ln can be precisely quantified in a matrix-independent way using inductively coupled plasma mass spectrometry (ICPMS) with the features of high sensitivity (down to ppt level) and element/isotope-specific subunit mass-resolved selectivity as well as isotope-dilution based accuracy. Integration of an Ln-cored complex and a targeting 'warhead' (such as small molecular inhibitor and/or homing peptide as well as antibody) should be expected to provide duplex signals (luminescence and element/isotope-specific mass) and, especially the quantitative information of targeted biomolecules can be obtained via accurate ICPMS determination of the element/isotope tagged in a conventional liquid biopsy, even their host circulating tumor cells (CTCs) when the biomolecules are cell membrane-spanning proteins. We thus designed and fabricated such a reporter consisting of an neodymium (Nd)-cored 1,4,7,10-tetraazacyclododecane-1,4,7-trisacetic acid (DOTA) complex together with a light-harvesting aminofluorescein (AMF) antenna moiety (AMF-DOTA-Nd) (**1** in Figure 1). Moreover, prostate-specific membrane antigen (PSMA), a prostate cancer biomarker,[15,16] is set as an example of targeted biomarkers in this study. PSMA is a 100 kDa type II transmembrane glycoprotein expressed in prostate epithelial cells with an internal portion of 19 amino acids (AAs), a transmembrane portion of 24 AAs, and a 707 AAs external portion.[17]

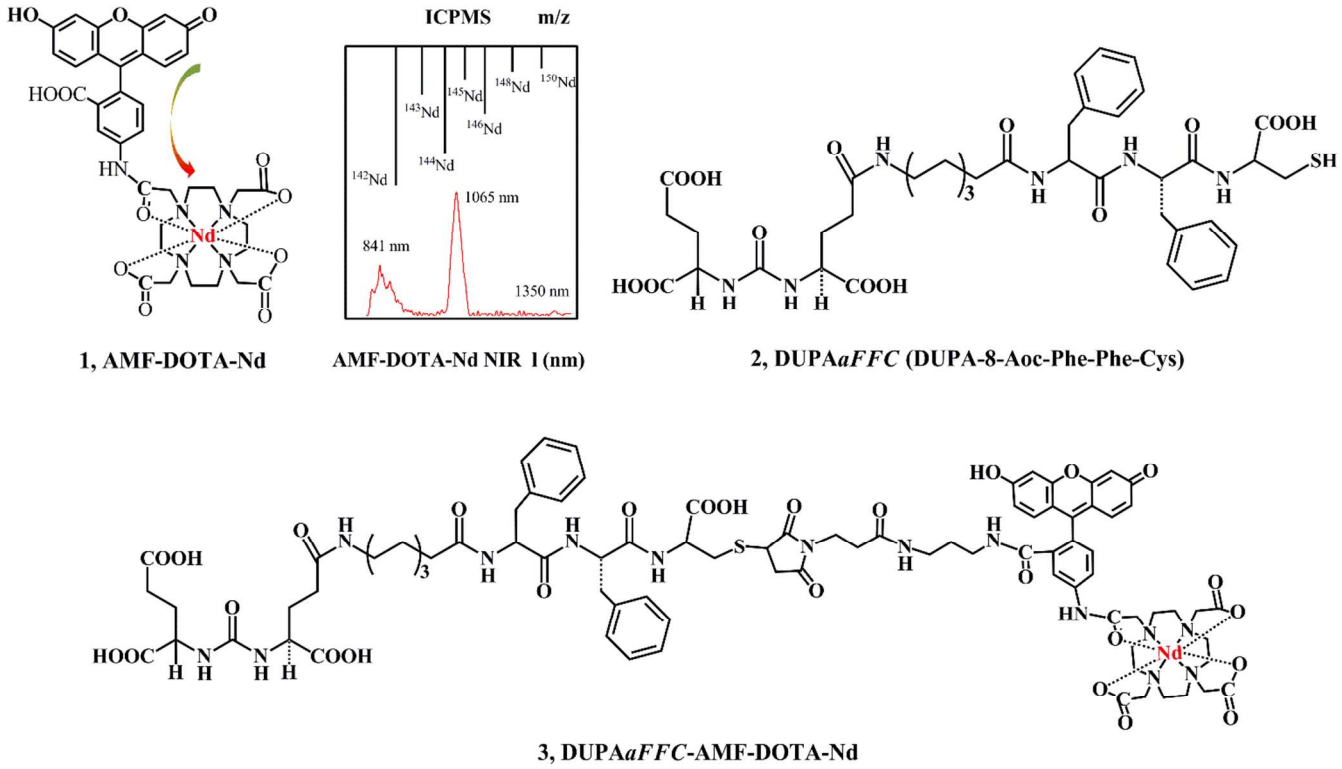

Figure 1. Structure of PSMA-targeting DUPA*aFFC*-AMF-DOTA-Nd tag. The antenna moiety AMF absorbs exciting light (494 nm), and then transfer the energy to DOTA-Nd, emitting NIR light (841 nm, 1065 nm and 1350 nm). In addition, the core Nd can be accurately quantified using ICPMS to obtain the mass spectrometric signals with its isotopic distribution of ^{142}Nd (27.2 %), ^{143}Nd (12.2 %), ^{144}Nd (23.8 %), ^{145}Nd (8.3 %), ^{146}Nd (17.2 %), ^{148}Nd (5.7 %) and ^{150}Nd (5.6 %). Peptidomemitic DUPA*aFFC* can specifically target PSMA.

The external portion can be specifically targeted by a urea-based peptidomimetic inhibitor,[18] such as 2-[3-(1,3-dicarboxypropyl)-ureido]pentanedioic acid (DUPA)-X (X denotes a peptide spacer).[19,20] Here, we synthesized DUPA-8-Aoc-Phe-Phe-Cys (DUPA*aFFC*; *aFFC* denotes 8-Aoc-Phe-Phe-Cys) (**2** in Figure 1), and covalently linked it to AMF-DOTA-Nd to obtain a nonradioactive NIR- and Nd-integrated DUPA*aFFC*-AMF-DOTA-Nd tag (**3** in Figure 1), targeting PSMA and PSMA-positive CTCs in blood in order to demonstrate the feasibility of the specific and duplex quantitative bioanalysis proposed.

Experimental Section

Materials and Instrumentations. All chemicals used in this study are of analytical grade or better without further purification. The ultrapure water used was prepared with a Milli-Q system (Millipore Filter Co., Bedford, MA). 3-maleimidopropionic acid, N-Boc-1,3-propane diamine, 5-aminefluorescein, N,N-diisopropylethylamine (DIPEA), O-(7-azabenzotriazol-1-yl)-N,N,N',N'-tetramethyluronium hexafluorophosphate (HATU), 10 % Pd/C and chloroacetyl chloride ($ClCH_2COCl$) were bought from J&K Scientific Ltd. (Beijing, China); 1,4,7-tri(t-butyl acetate) 1,4,7,10-tetraazacyclododecane (DO3A-tBu ester) was purchased from Macrocyclics (Dallas, TX); L-glutamate di-tert-butyl ester and H-L-Glu(OBn)-OtBu used for building the DUPA*aFFC*-AMF-DOTA were purchased from Maya Reagent Inc. (Zhejiang, China). Triphosgene, neodymium oxide (Nd_2O_3, purity > 99.9 %) and silica gel (300-400 mesh) were obtained from Aladdin Reagent Inc. (Shanghai, China); ^{154}Sm-enriched Sm_2O_3 (> 99 %) was purchased from Cambridge Isotope Laboratories, Inc. (Andover, MA, USA). Trifluoroacetic acid (TFA), acetonitrile (ACN) and methanol used as the components of chromatographic mobile phases were obtained from Sigma-Aldrich (St. Louis, MO). Recombination human PSMA (PSMA) was obtained from R&D Systems Inc. (Minneapolis, USA). Prostate cancer cell lines, LNCaP (lymphatic metastatic prostatic adenocarcinoma, PSMA-positive), DU145 (brain metastatic of prostatic adenocarcinoma, PSMA-negative) and PC-3 (bone metastatic prostatic adenocarcinoma, PSMA-negative) were obtained from the Cell Line Bank of the Shanghai Institute for Biological Science (China). RPMI-1640 culture fluid, fetal bovine serum, penicillin and streptomycin used for cell culture were obtained from Gibco (Waltham, USA). Dialysis membranes (molecular weight cut off, 8 kDa) were purchased from Sangon Biotech Co., Ltd. (Shanghai, China). The blood samples were obtained from the Affiliated Zhongshan Hospital of Xiamen University. They include 45 blood samples from PCa patients, 20 benign prostatic hyperplasia (BPH) patients, 8 men and 7 women healthy volunteers (detailed information were listed in Table S1). All the blood samples were stored at -80 °C until use. These obtained samples were approved by the ethics committee, and the patients signed the informed consents.

An ESI ion trap mass spectrometer (ESI-IT-MS) (Esquire-LC, Bruker Daltonics, Bremen, Germany) was used for measuring molecular weight and chemical composition of the synthesized molecules. The operational parameters were as follows: nebulizer, 20 psi; dry gas, 8 L/min; dry temperature, 300 °C; capillary voltage, 3.0 KV. HPLC analysis were performed using an Agilent 1100 series chromatographic system (Agilent Technologies, Palo Alto, CA) equipped with a G1365B-MWD UV detector (190 - 600 nm) and a ZORBAX

300SB-C18 column (2.1 I.D. × 100 mm in length, 3.5 μm particle size). Preparative HPLC purification of the compounds synthesized was performed using a Shimadzu 10AD HPLC system with an SPD-M10Avp detector and an Elite Hypersil BDS C18 column (10.0 I.D. × 250 mm in length, 5 μm particle size). Silica gel column chromatography for purification of the compounds was performed using silica gel (300-400 mesh) in a 3 I.D × 150 cm in length glass column (Beijing Synthware Glass, China). NMR spectrum was acquired on a Varian Gemin-400 NMR instrument (400 MHz). Hitachi U3900 spectrophotometer and F7000 fluorescence spectrometer, Edinburgh FLS980 spectrometer (200 to 2500 nm) and Zeiss LSM780 laser confocal scanning microscope (LCSM) (350 to 800 nm) were used for measuring UV-visible absorption spectrum, fluorescence spectrum, near infrared luminescence spectrum, fluorescence lifetime and cell imaging. Beckman Coulter FC500 was used for counting cells. For stable Nd isotope analysis, an ELAN DRC II ICPMS (PerkinElmer, SCIEX, Canada) equipped with a concentric pneumatic nebulizer and a cyclonic spray chamber. The ICPMS operational parameters were as follows: nebulizer Ar gas, 0.88 L/min; auxiliary Ar gas, 1.0 L/min; plasma Ar gas, 15 L/min; RF power, 1200 W; dwell time, 100 ms; lens voltage, 7.2 V. Parameters such as Ar nebulizer gas flow and lens voltage were optimized daily to obtain the best sensitivity with ELAN DRC II Setup/Stab/Masscal Solution. It was coupled to size exclusion chromatography (SEC) (SEC-ICPMS) in order to confirm the specificity and stoichiometry of DUPA*aFFC*-AMF-DOTA-Nd toward PSMA, in which Superdex 75 10/300 GL column was used and ^{142}Nd was monitored. We also investigated the interactions between DUPA*aFFC*-AMF-DOTA-Nd and BSA (66 kDa, Sigma) and/or cytochrome C (13 kDa, Sigma) using SEC-ICPMS.

Synthesis of DUPA*aFFC*-AMF-DOTA-Nd. The synthetic route is illustrated in Scheme S1 in the Supporting Information. To link AMF and DOTA, we first derivatized 5-aminefluorescein into 5-chloromethylamidofluorescein (75 % yield) using $ClCH_2COCl$ in acetone at room temperature for 5 h. It was then conjugated with DO3A-tBu ester via a typical nucleophilic substitution for 9 h using K_2CO_3 as an acid binding agent, KI as a stabilizing agent and DMF as a solvent under an anhydrous anaerobic condition at 80 ºC,[21] so as to obtain AMF-DOTA-tBu (40 %). After tBu was deprotected from AMF-DOTA-tBu using TFA, the resulted AMF-DOTA was mixed with excess Nd^{3+} in ammonium acetate buffer (pH 6.4) at 37 ºC for 3 h to obtain AMF-DOTA-Nd (**1** in Figure 1). 3-maleimidopropionic acid reacted with N-Boc-1,3-propane diamine, and then used TFA for deprotecting Boc to obtain N-(3-aminopropyl)-3-maleimidopropanamide (56 %). It contains both $-NH_2$ and maleimido group serving as a linker between AMF-DOTA-tBu and the peptidomimetic guiding moiety. Aminolysis of AMF-DOTA-tBu using N-(3-aminopropyl)-3-maleimidopropanamide and then deprotection of tBu resulted in MMA-AMF-DOTA (14 %). In parallel, synthesis of the peptidomimetic guiding moiety started from L-glutamate di-tBu to react with triphosgene for 2 h using triethylamine (TEA) as an acid binding agent at -78 °C under anhydrous anaerobic condition, and then a solution of H-L-Glu(OBn)-OtBu together with TEA in DCM was added to react at room temperature overnight to synthesize 2-[3-(3-benzyloxycarbonyl-1-tert-butoxycarbonyl-propyl)-ureido]pentanedioic acid ditert-butyl ester (77 %). After deprotecting benzyl group using 10 % Pd/C, we obtained 2-[3-(1,3-bis-tert-butoxycarbonyl-propyl)-ureido]pentanedioic acid-tert-butyl ester (DUPA-tBu) (68 %). The peptidomimetic DUPA*aFFC* (**2** in Figure 1) was obtained through solid phase peptide synthesis using DUPA-tBu, 8-Aoc (*a*), Phe (*F*), and Cys (*C*) as starting materials.[19] Subsequently, the typical Michael addition between the sulfhydryl in DUPA*aFFC* and maleimido group in MMA-AMF-DOTA was subjected to react for 2 h in ammonium acetate buffer (pH 6.4) at 37 °C, resulting in DUPA*aFFC*-AMF-DOTA (97 % yield). Finally, we obtained DUPA*aFFC*-AMF-DOTA-Nd (**3** in Figure 1) after coordination of Nd^{3+} into DUPA*aFFC*-AMF-DOTA. The stability constant (log *K*) of DOTA-Nd is high up to 23,[22] ensuring the stability of Nd^{3+} in DUPA*aFFC*-AMF-DOTA-Nd during labeling PSMA process. All the compounds synthesized were characterized using HPLC/ESI-IT-MS and ^{1}HNMR after purification using the preparative HPLC or silica gel column chromatography (see Figures S1-S19 and the detailed procedures in the Supporting Information).

Total PSMA (*t*PSMA), plasmic PSMA (*p*PSMA) and membrane-spanning PSMA (*m*PSMA) measurements. Prior to quantification of PSMA in blood, the samples were appropriately diluted with PBS buffer. *t*PSMA in the blood sample (1 mL) was determined using ICPMS and NIR after 3 h incubation at 37 °C with DUPA*aFFC*-AMF-DOTA-Nd (2 μL, 5 mM) and dialyzing out the excess free DUPA*aFFC*-AMF-DOTA-Nd. After the blood sample was subjected to centrifuge (2630 g, 5 min) to separate the blood plasma and cells, *p*PSMA and *m*PSMA were determined in the plasma and the residual cells.

Cell labeling and counting. The three kinds of prostate cancer cell lines, LNCaP (PSMA-positive), PC-3 (PSMA-negative) and DU145 (PSMA-negative),[23] which were cultured in RPMI-1640 medium containing 10% heat-inactivated fetal bovine serum, 1% penicillin, and 1% streptomycin at 37 °C in a 5 % CO_2 : 95 % air incubator, were used to investigate the cell specificity of DUPA*aFFC*-AMF-DOTA-Nd. Each kind of cells was seeded in a 12-well plate (10^5 cells per well) and incubated overnight at 37 °C. After washing, 20 μL 50 nM DUPA*aFFC*-AMF-DOTA-Nd, DUPA*aFFC*-AMF-DOTA, AMF-DOTA-Nd and PBS buffer (blank) were added respectively into the first four-wells of the 12-well plate for 3 h. At least, triplicate such runs were performed. After washing three times with PBS buffer, the trypsinized off-well cells in the first four-wells were dissolved in ultrapure concentrated HNO_3 overnight, and appropriately diluted prior to determination using ICPMS; the trypsinized off-well cells in the second four-wells were dissolved in PBS buffer for direct NIR measurement; the cells in the last four-wells were fixed with 4 % paraformaldehyde for 15 min at 4 ºC and stained cell nucleus with 4',6-diamidino-2-phenylindole (DAPI, λ_{em} = 461 nm, blue), in addition to DUPAa*FFC*-AMF-DOTA-Nd, DUPAa*FFC*-AMF-DOTA, AMF-DOTA-Nd and PBS buffer, for imaging the cell nucleus and *m*PSMA on the surface of the cells using LCSM. To further confirming the specificity of the probe towards PSMA-positive cancer cells, blocking studies were performed. LNCaP cells were pre-incubated with 50 nM DUPA*aFFC* for 3 h prior to the addition of 50 nM DUPAa*FFC*-AMF-DOTA-Nd and/or DUPA*aFFC*-AMF-DOTA. Moreover, for counting PSMA-positive LNCaP cells using ICPMS and NIR, 20 μL 50 nM DUPAa*FFC*-AMF-DOTA-Nd was added to a series known number of LNCaP cells. After 3 h incubation, washing three times with PBS buffer to get rid of the excess free DUPA*aFFC*-AMF-DOTA-Nd prior to measurements.

Results and discussion

Spectroscopic characteristics of DUPA*aFFC*-AMF-DOTA-Nd. In order to evaluate the NIR luminescent and mass spectroscopic properties of DUPA*aFFC*-AMF-DOTA-Nd, we first investigated the optical properties of DUPA*aFFC*-AMF-DOTA-Nd, DUPA*aFFC*-AMF-DOTA and AMF as well as $Nd(NO_3)_3$. AMF, DUPA*aFFC*-AMF-DOTA and DUPA*aFFC*-AMF-DOTA-Nd had the same absorption peak at 494 nm (Figure S20). Under the excitation of 494 nm, AMF and DUPA*aFFC*-AMF-DOTA emitted the same fluorescence peak at 520 nm from AMF with the lifetime of 5.7 ns as expected; while the NIR luminescence of DUPA*aFFC*-AMF-DOTA-Nd was observed at 841 nm ($^4F_{3/2} \rightarrow {}^4I_{9/2}$), 1065 nm ($^4F_{3/2} \rightarrow {}^4I_{11/2}$) and 1350 nm ($^4F_{3/2} \rightarrow {}^4I_{13/2}$),[24,25] with the longer lifetime of 2.5 μs and much bigger 'stokes shift' of 347 nm, 571 nm and 856 nm (Figure 2), suggesting the successful energy transfer from AMF to DOTA-Nd. In the case of $Nd(NO_3)_3$, neither noticeable absorption at 494 nm nor luminescence from visible to NIR could be recorded due to the very low molar absorption coefficient of Nd^{3+} arising from the parity-forbidden transition of f-orbital electron and its relatively small diameter.[26] All these results confirmed the crucial role of AMF for the NIR emission from Nd^{3+} in DUPA*aFFC*-AMF-DOTA-Nd. It absorbs the matched energy with parity-allowed transition at the triplet state, which transformed from the singlet state of the excited AMF via intersystem crossing. We then measured a series of DUPA*aFFC*-AMF-DOTA-Nd solutions of different concentrations from 0 to 257.5 nM (corresponding to 0.5 μg/mL) to make a calibration curve at 1065 nm considering that it is strongest among the three NIR luminescence (Figure 3). The linear dynamic range was from 0.1 to 103 nM (corresponding to 0.2 to 200 ng/mL) (correlation coefficient $R^2 = 0.992$), and the limit of detection (LOD, 3σ) reached 77.2 pM (corresponding to 0.15 ng/mL) with an RSD of 1.4 % at 76.4 ng/mL (n = 5). Subsequently, the mass spectroscopic property of DUPA*aFFC*-AMF-DOTA-Nd was investigated using ICPMS monitoring ^{142}Nd and, ^{154}Sm as species-unspecific isotopic internal standard. Nd has much lower first ionization potential (ca. 5.5 eV) compared with that (15.8 eV) of Ar, which is used as the plasma gas in ICP, resulting in almost 100 % ionization efficiency and thus very low LOD on an conventional Ar-based ICPMS.[27] The obtained results indicated that DUPA*aFFC*-AMF-DOTA-Nd and $Nd(NO_3)_3$ had the same mass spectrometric signal intensity at equal Nd concentration (Figure 3), demonstrating a species-independent ICPMS response due to ICP is a very hard ionization source. The LODs (3σ), when monitoring ^{142}Nd (its abundance is 27.2 %, the highest one among Nd isotopes), was down to 2.8 pM (corresponding to 5.4 pg/mL), almost 28-fold lower than that of the NIR measurement; and the linear dynamic range was up to 257.5 nM DUPA*aFFC*-AMF-DOTA-Nd (corresponding to 500 ng/mL; higher concentrations were not tested) ($R^2 = 0.997$) with an RSD of 0.5 % at 10.4 ng/mL (n = 7). All the results suggested that both the NIR luminescence and ICPMS signals could be obtained from the same Nd-cored DUPA*aFFC*-AMF-DOTA-Nd. Compared with the trifunctional probe ($\lambda_{ex/em}$ = 494/520 nm; ^{153}Eu) that we previously designed and synthesized, in which AMF and DOTA-Eu worked separately;[28] and the AuNP-quenched activity-released Eu-BCTOT-peptide probe ($\lambda_{ex/em}$ = 350/614 nm; ^{153}Eu) that worked by the mediation of a protease,[29] DUPA*aFFC*-AFM-DOTA-Nd is an Nd-cored second NIR- and mass-integrated duplex tag ($\lambda_{ex/em}$ = 494/1065 nm; ^{142}Nd).

Selectivity of DUPA*aFFC*-AMF-DOTA-Nd toward PSMA. In addition to the readout properties, the targeting feature of DUPA*aFFC*-AMF-DOTA-Nd is another important

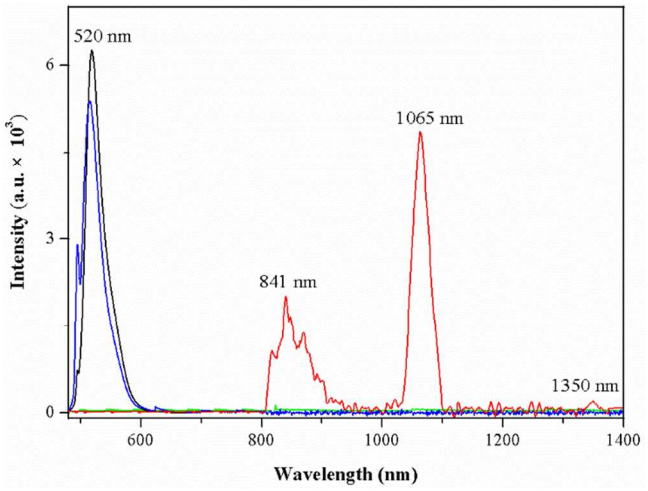

Figure 2. Emission spectra of $Nd(NO_3)_3$ (green line), AMF (black line), DUPA*aFFC*-AMF-DOTA (blue line), DUPA*aFFC*-AMF-DOTA-Nd (red line) of 10.0 μM each in 20 mM PBS buffer (pH 7.4). Two-step scanning from 450 nm to 800 nm (visible region) and then 800 nm to 1500 nm (NIR region) was performed under the excitation of 494 nm.

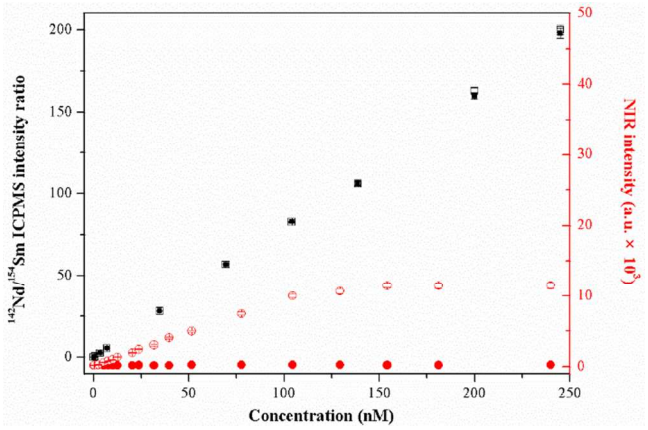

Figure 3. ICPMS and NIR responses from a series of $Nd(NO_3)_3$ (black solid square for ICPMS, red solid circle for NIR) and DUPA*aFFC*-AMF-DOTA-Nd (black open square for ICPMS, red open circle for NIR) solutions (0 - 250 nM), respectively.

factor for achieving a specific quantification of PSMA and counting its host CTCs. According to the previous studies,[30-32] DUPA-X-Dap-Asp-Cys (Dap denotes *β*-L-diaminopropionic acid) interacts with the external domain of PSMA molecule with 1:1 stoichiometry with high affinity (K_d = 14 nM).[19,33] The carbonyl oxygen of Glu-C(O)- Glu in DUPA was found to coordinate directly with the zinc in the active site located at the bottom of S1 pocket domain of PSMA, the α and α′-carboxyl interacting with Arg210 and Arg534, and the γ-carboxyl forming a third salt bridge with Lys699 as autodocked in Figure S21. Moreover, additional hydrophobic and hydrogen bonding interactions from the two Phe and ureal nitrogen in DUPA-8-Aco-Phe-Phe-Dap-Asp-Cys with S1 pocket were proved to reinforce the affinity of DUPA-8-Aco-Phe-Phe-Dap-Asp-Cys to PSMA.[19] In order to prove the labeling efficiency of DUPA*aFFC*-AMF-DOTA-Nd tag, which was designed and synthesized in this study, toward PSMA, we used SEC that is able to separate the molecules of different weights and/or sizes, together with ICPMS for monitoring ^{142}Nd. The results obtained (Figure 4) indicated that a new peak appeared at 9.5 min in the case of mixing PSMA (5 nM) with DUPA*aFFC*-AMF-DOTA-Nd (15 nM) in 100 μL 50 mM PBS buffer (pH 7.4), in addition to

the peak at 19.4 min compared with DUPA*aFFC*-AMF-DOTA-Nd (15 nM) alone. The new peak was PSMA-DUPA*aFFC*-AMF-DOTA-Nd because of its much larger molecular weight thus eluted earlier from the SEC, and the determination of ^{142}Nd as well. Moreover, the peak area ratio was 2:1 (19.4 min to 9.5 min), and the sum of them equaled to that of DUPA*aFFC*-AMF-DOTA-Nd alone. This observed fact suggested that not only complete tagging of PSMA by DUPA*aFFC*-AMF-DOTA-Nd, but also the stoichiometry is 1:1. Selectivity of DUPA*aFFC*-AMF-DOTA-Nd was also investigated using other model proteins such as BSA and cytochrome C together with PSMA. No DUPA*aFFC*-AMF-DOTA-Nd tagged BSA and cytochrome C were detected, indicating its specificity toward PSMA (Figure S22). In this way, the LOD (3σ) was down to 2.9 pM PSMA (corresponding to 0.3 ng PSMA/mL) with a linear dynamic range up to 245 nM (corresponding to 25 μg/mL, $R^2 = 0.995$; higher concentrations were not tested) with an RSD of 1.5% at 61.1 ng/mL (n = 10) using ICPMS. While the linear range obtained was from 0.1 to 98 nM (corresponding to from 10 ng/mL to 10 μg/mL, $R^2 = 0.990$) (Figure S23), and the LOD (3σ) was 95 pM PSMA (corresponding to 9.7 ng PSMA/mL) using NIR at 1065 nm with an RSD of 3.5 % at 61.1 ng/mL (n = 5). Comparing to NIR, the LOD of PSMA using ICPMS is almost 33 times lower, and the sensitivity remains almost unchanged as that of DUPA*aFFC*-AMF-DOTA-Nd itself, indicating again the matrix-independent advantage of ICPMS. When compared with the sensitivities obtained from the western blot using fluorescent detection and ProteinChip arrays (about 1 μg/mL) with surface-enhanced laser desorption/ionization time-of-flight mass spectrometry,[34,35] the LOD obtained using ICPMS in this study is much lower; and comparable to those of fluorescence-based dual-monoclonal sandwich assay (less than 1 ng/mL) and electrochemical microfluidic immunoarray (0.15 pg/mL) with additional enrichment procedures.[36,37]

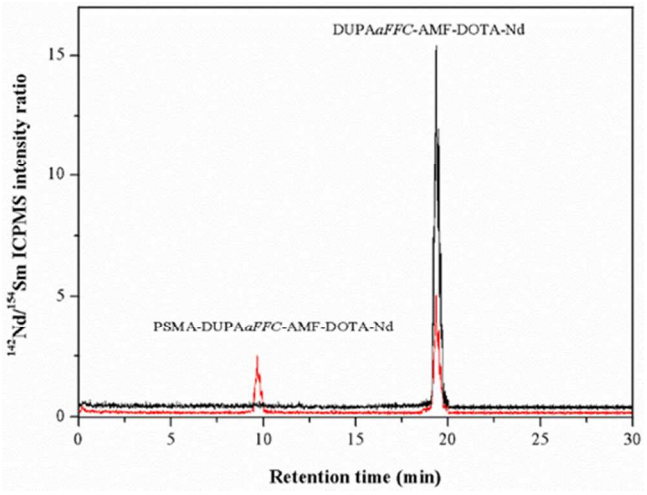

Figure 4. SEC-ICPMS chromatograms of DUPA*aFFC*-AMF-DOTA-Nd (15 nM) (black line) and, the mixture of PSMA (5 nM) with DUPA*aFFC*-AMF-DOTA-Nd (15 nM) (red line). ^{142}Nd was monitored; a Superdex 75 10/300 GL column (10 mm I.D. × 300 mm in length) and 50 mM ammonium bicarbonate (pH 7.4) mobile phase with the flow rate of 0.8 mL/min were used.

Specificity of DUPA*aFFC*-AMF-DOTA-Nd toward PSMA-positive cells. In order to examine the tagging specificity of DUPA*aFFC*-AMF-DOTA-Nd toward cells, we used LNCaP (PSMA-positive), DU145 (PSMA-negative) and PC-3 (PSMA-negative) cell lines. Because we did not have an second NIR window microscopy at hand this moment (although PSMA-DUPA*aFFC*-AMF-DOTA-Nd could be determined using an Edinburgh FLS980 fluorescence spectrophotometer at 1065 nm), DUPA*aFFC*-AMF-DOTA-Nd and/or DUPA*aFFC*-AMF-DOTA that emits green fluorescence at 520 nm owing to the absence of Nd^{3+} were used in parallel to quantify and visualize the DUPA*aFFC*-targeted PSMA-positive cells using ICP-MS and under a conventional LCSM. The results obtained indicated that the PSMA-positive LNCaP cells could be counted using ICPMS (Figure S24a_1) and NIR (Figure S24a_2) with DUPA*aFFC*-AMF-DOTA-Nd, and could also be fluorescently detected (Figure S24a_2') and green-visualized (Figure S24a_4') at 520 nm when using DUPA*aFFC*-AMF-DOTA; but not when only PBS and AMF-DOTA-Nd without the targeting DUPA*aFFC* were used (Figure S24a_1''-a_5'' and a_1'''-a_5'''). In the cases of PSMA-negative DU145 and PC-3, either DUPA*aFFC*-AMF-DOTA-Nd and DUPA*aFFC*-AMF-DOTA or AMF-DOTA-Nd and PBS did not give any detectable signals (Figure S24b_1-b_5, b_1'-b_5', b_1''-b_5'', b_1'''-b_5''' and c_1-c_5, c_1'-c_5', c_1''-c_5'', c_1'''-c_5'''), suggesting the specificity of DUPA*aFFC*-AMF-DOTA-Nd and DUPA*aFFC*-AMF-DOTA toward the PSMA-positive LNCaP cell. Moreover, when we used DUPA*aFFC* to block the LNCaP cell membrane-spanning *m*PSMA prior to the addition of DUPA*aFFC*-AMF-DOTA-Nd and/or DUPA*aFFC*-AMF-DOTA, neither ICPMS and NIR luminescent and/or green fluorescent signals nor green-visualization could be observed (Figure S24a_1''''-a_5''''), again confirming the specificity of this tag toward the PSMA-positive LNCaP cell. Subsequently, different number of the LNCaP cells ranging from 5×10^2 to 5×10^5 that were counted by flow cytometry was labeled with DUPA*aFFC*-AMF-DOTA-Nd tag for quantifying the amount of *m*PSMA expressed per LNCaP cell (Figure 5). The results obtained indicated that one LNCaP cell expressed $(3.6 \pm 0.1) \times 10^7$ (ICPMS) and $(3.6 \pm 0.2) \times 10^7$ (NIR) *m*PSMA molecules in the case that 5×10^4 LNCaP cells were employed, taking the molecular weight of PSMA (100 kDa) into account. It should be noted that ICPMS gave similar results even the cell number was 5×10^2, but not the case when using NIR owing to its lower detection limit. On the basis of the LOD of PSMA, down to 48 and 1596 LNCaP cells could be counted directly using ICPMS and NIR together with DUPA*aFFC*-AMF-DOTA-Nd. Considering the Avogadro constant saying that one mole contains 6.023×10^{23} particles, the cell-counting sensitivity theoretically reached 8.0×10^{-23} (ICPMS) and 2.6×10^{-21} (NIR) mole level. Compared to NIR, ICPMS was superior in either the matrix-independent m/z signals or 33 times higher sensitivity.

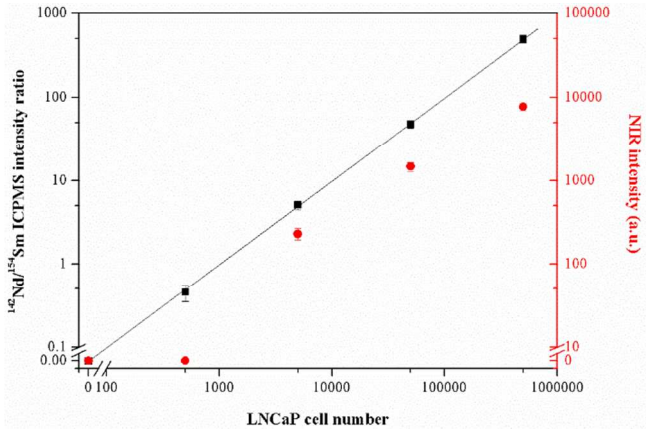

Figure 5. Relationship between the LNCaP cell number and the intensity of ICPMS (black square) or NIR (red circle). Log 10

scale was used after the break (x axis break from 1 to 100, Y axis for ICPMS from 0.01 to 0.1, for NIR from 1 to 100) at 5% of the axis.

PSMA in blood samples. Before applying the method developed here to the real blood samples, we were aware that PSMA has its splice variants such as PSM', PSM-C, PSM-D and PSM-E.[38-41] All these variants have the same DUPA*aFFC* targeting domain, thus the determined amount in the blood samples should be the sum of PSMA and its splice variants. It was termed as total PSMA (*t*PSMA) as shown in Figure 6 (detailed data are listed in Table S1). *t*PSMA determined in PCa blood samples ranged from 295.4 to 2605.1 ng/mL, the mean and median values were 800.7 ng/mL and 676.8 ng/mL. When analyzing these data (the mean value of Gleason score 6, 569.3 ng/mL; 7, 622.7 ng/mL; 8, 730.8 ng/mL; 9, 1781.1 ng/mL), we could see that the *t*PSMA not only increased along with their Gleason score, but also were significantly higher than those of BPH blood samples from 193.3 to 454.3 ng/mL, 317.4 ng/mL (mean) and 309.0 ng/mL (median) ($P < 0.001$). Thus, 320 ng/mL might be roughly thought as a threshold value to differentiate BPH and PCa; and 600 ng/mL could be a threshold value for diagnosis of PCa according to Gleason score 6 that is thought to be a definite PCa.[42]. By comparison, *t*PSMA in the blood samples of healthy men and women were much lower, ranging from 152.4 to 362.5 ng/mL and 30.4 to 49.3 ng/mL, with the mean values of 231.0 and 38.9 ng/mL, and median values of 222.4 and 40.1 ng/mL ($P < 0.001$).

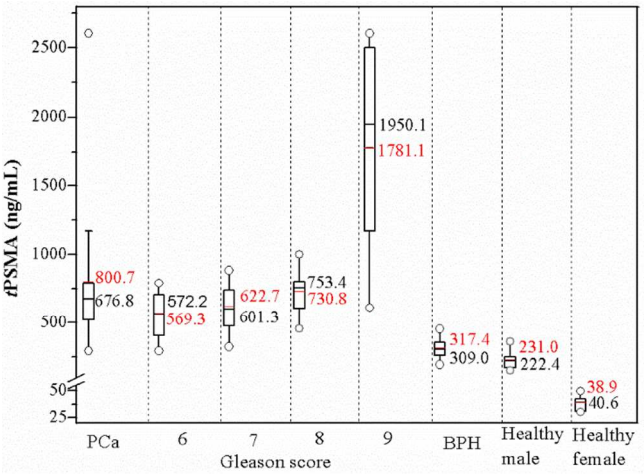

Figure 6. Boxplots of *t*PSMA concentrations in the PCa with different Gleason score, BPH, healthy male and female blood samples. The boxes represent the 25th and 75th percentiles; the whiskers represent the 5th and 95th percentiles; and outliers are displayed by circles. The black lines represent the median value; the red lines represent the mean value.

Counting PSMA-positive CTCs. Among PSMA and its splice variants, only PSMA and PSM-E are known as the transmembrane proteins anchoring on its host cells,[43] *m*PSMA; while the other plasmic variants including PSM', PSM-C and PSM-D (termed as *p*PSMA here) are either inside or out of the cells entering into the blood circulation.[38] To simplify counting the PSMA-positive CTCs in the real PCa blood samples, we centrifuged out the plasma, where *p*PSMA exist. Afterwards, we counted the PSMA-positive CTCs in the six PCa blood samples selected (1 mL each) of different Gleason scores via the determination of *m*PSMA in the blood residues containing the blood cells using ICPMS together with DUPA*aFFC*-AMF-DOTA-Nd tag (Table 1). Results obtained indicated that there were 134 to 773 PSMA-positive CTCs within 20 % RSD in the blood samples along with the increase in the Gleason score from 6 to 9, being in accordance to the fact that CTCs are within 1000 in 1 mL blood.[43-46] It is worth noting that PSM-E, in addition to PSMA, also contribute to *m*PSMA, the counted CTCs here should be more accurate than those merely based on the amount of PSMA expressed on the cells, considering PSMA and PSM-E have a similar molecular weight according to their mRNA.[41] Clearly, results of counting CTCs would be much more accurate when a more specific membrane-spanning biomarker without the splice variants was targeted in the near future.

Table 1. The concentrations of *t*PSMA, *p*PSMA and *m*PSMA, and the number of PSMA-positive CTCs in the six selected PCa blood samples of different Gleason score[a]

No.	Age	Gleason score	*t*PSMA in blood (ng/mL)	*p*PSMA in plasma (ng/mL)	*m*PSMA in cells (ng/mL)	cell number (copy)
1	50	6	324.6 ± 4.4	323.8 ± 3.6	0.8 ± 0.1	134 ± 17
2	75	6	741.5 ± 7.9	740.6 ± 8.5	1.0 ± 0.2	168 ± 33
3	63	7	792.3 ± 10.1	790.1 ± 6.8	2.2 ± 0.3	367 ± 50
4	60	7	753.4 ± 5.7	750.8 ± 7.4	2.5 ± 0.3	420 ± 50
5	78	8	1003.6 ± 10.2	1000.4 ± 7.1	3.4 ± 0.4	571 ± 68
6	83	9	2500.2 ± 15.2	2495.6 ± 14.3	4.6 ± 0.4	773 ± 68

a, each sample was measured three times.

Conclusions

We designed and synthesized an NIR luminescent (1065 nm) and mass spectroscopic (^{142}Nd) duplex AMF-DOTA-Nd tag. When it covalently linked with a PSMA-targeting peptidomimetic 'warhead', DUPA*aFFC*, DUPA*aFFC*-AMF-DOTA-Nd demonstrated its ability as a specific duplex readout probe, exemplified in the quantification of *t*PSMA in the PCa, BPH and healthy blood samples using ICPMS. The *t*PSMA concentration in blood can be used as an index to not only diagnose PCa (threshold value, 600 ng/mL) but also differentiate BPH from PCa (320 ng/mL); moreover, hundreds of PSMA-positive CTCs in the PCa blood samples were counted via *m*PSMA using ICPMS. If having a second NIR window microscopy at hand, we believe that NIR-imaging of *m*PSMA and its host CTCs would become reality. Future work will be focused on the modification of the NIR Nd-tag with other targeting groups to expand its application to the quantification and counting of different biomarkers and CTCs.

ASSOCIATED CONTENT

Supporting Information

The Supporting Information is available free of charge on the ACS Publications website.

Synthesis and characterization of DUPA*aFFC*-AMF-DOTA-Nd, UV-Vis absorption spectra, Autodocking, SEC-ICP-MS, calibration cures of PSMA using ICPMS and NIR together with DUPA*aFFC*-AMF-DOTA-Nd tag, specificity of DUPA*aFFC*-AMF-DOTA-Nd toward PSMA-positive cells, results of total PSMA in real blood samples (PDF)

AUTHOR INFORMATION

Corresponding Author

* E-mail: qqwang@xmu.edu.cn; Fax: +86 (0)592 2187400.

* E-mail: baipeiming@xmu.edu.cn

ORCID
Qiuquan Wang: 0000-0002-5166-4048

Notes
The authors declare no competing financial interest.

ACKNOWLEDGMENTS
This work was financially supported by the National Natural Science Foundation of China (Grants 21535007, 21475108, 21275120), the National Basic Research 973 Program (Grant 2014CB932004) and National Science and Technology Basic Work (2015FY111400), as well as the Foundation for Innovative Research Groups of the National Natural Science Foundation of China (Grant 21521004), Program for Changjiang Scholars and Innovative Research Team in University (PCSIRT, Grant IRT13036).

REFERENCES

(1) Fernández-Suárez, M.; Ting, A. Y. *Nat. Rev. Mol. Cell Biol.* **2008**, *9*, 929-943.
(2) Kobayashi, H.; Ogawa, M.; Alford, R.; Choyke, P. L.; Urano, Y. *Chem. Rev.* **2010**, *110*, 2620–2640.
(3) Terai, T.; Nagano, T. *Eur. J. Physiol.* **2013**, *465*, 347–359.
(4) Giepmans, B. N. G.; Adams, S. R.; Ellisman, M. H.; Tsien, R. Y. *Science*, **2006**, 312, 217-224.
(5) König, K. *J. Microsc.* **2000**, *200*, 83–104.
(6) Bünzli, J. C. G.; Eliseeva, S. V. *J. Rare Earths,* **2010**, *28*, 824-842.
(7) He, H. S. *Coor. Chem. Rev.* **2014**, *273–274*, 87–99.
(8) Bünzli, J. C. G. *Chem. Rev.* **2010,** *110,* 2729–2755.
(9) Zhou, J.; Ma, H. M. *Chem. Sci.* **2016**, *7*, 6309-6315.
(10) Duimstra, J. A.; Femia, F. J.; Meade, T. J. *J. Am. Chem. Soc.* **2005**, *127*, 12847-12855.
(11) Tremblay, M. S.; Zhu, Q.; Martı´, A. A.; Dyer, J.; Halim, M.; Jockusch, S.; Turro, N. J.; Sames, D. *Org. Lett.* **2006**, *8*, 2723-2726.
(12) Tremblay, M. S.; Sames, D. *Chem. Commun.* **2006**, *39*, 4116-4118.
(13) Tremblay, M. S.; Halim, M.; Sames, D. *J. Am. Chem. Soc.* **2007**, *129*, 7570-7577.
(14) Dai, Z. C.; Tian, L.; Ye, Z. Q.; Song, B.; Zhang, R.; Yuan, J. L. *Anal. Chem.* **2013**, *85*, 11658-11664.
(15) Israeli, R. S.; Powell, C. T.; Fair, W. R.; Heston, W. D. W. *Cancer Res.*, **1993**, *53*, 227-230.
(16) Lütje, S.; Heskamp, S.; Cornelissen, A. S.; Poeppel, T. D.; van den Broek, S. A.; Rosenbaum-Krumme, S.; Bockisch, A.; Gotthardt, M.; Rijpkema, M.; Boerman, O. C. *Theranostics*, **2015**, *5*, 1388-1401.
(17) Chang, S. S. *Rev. Urol.* **2004**, *4*, 13-18.
(18) Kozikowski, A. P.; Nan, F. J.; Conti, P.; Zhang, J. Z.; Ramadan, E.; Bzdega, T.; Wroblewska, B.; Neale, J. H.; Pshenichkin, S.; Wroblewski, J. T. *J. Med. Chem.* **2001**, *44*, 298-301.
(19) Kularatne, S. A.; Zhou, Z. G.; Yang, J.; Post, C. B.; Low, P. S. *Mol. Pharmaceut.* **2009**, *6*, 790-800.
(20) Machulkin, A. E.; Ivanenkov, Y. A.; Aladinskaya, A. V.; Veselov, M. S.; Aladinskiy, V. A.; Beloglazkina, E. K.; Koteliansky, V. E.; Shakhbazyan, A. G.; Sandulenko, Y. B.; Majouga, A. G. *J. Drug Target.* **2016**, *24*, 679-693.
(21) Aita, K.; Temma, T.; Kuge, Y.; Saji, H. *Luminescence* **2007**, *22*, 455-461.
(22) Bünzli, J. C. G. *Acc. Chem. Res.* **2006**, *39*, 53-61.
(23) Laidler, P.; Dulińska, J.; Lekka, M.; Lekki, J. *Arch. Biochem. Biophys.* **2005**, *435*, 1-14.
(24) Heffern, M. C.; Matosziuk, L. M.; Meade, T. J. *Chem. Rev.* **2013**, *114*, 4496-4539.
(25) Hasegawa, Y.; Ohkubo, T.; Sogabe, K.; Kawamura, Y.; Wada. Y.; Nakashima, N.; Yanagida, S. *Angew. Chem., Int. Ed.* **2000**, *39*, 357-360.
(26) Bünzli, J. C. G. *Chem. Rev.* **2010**, *110*, 2729–2755.
(27) Wendt, K.; Gottwald, T.; Mattolat, C.; Raeder, S. *Hyperfine Interact.* **2014**, *227*, 55–67.
(28) Zhang, Z. B.; Luo, Q.; Yan, X. W.; Li, Z. X.; Luo, Y. C.; Yang, L. M.; Zhang, B.; Chen, H. F.; Wang, Q. Q. *Anal. Chem.* **2012**, *84*, 8946−8951.
(29) Feng, D.; Tian, F.; Qin, W. J.; Qian, X. H. *Chem. Sci.* **2016**, *7*, 2246–2250.
(30) Barinka, C.; Byun, Y.; Dusich, C. L.; Banerjee, S. R.; Chen, Y.; Castanares, M.; Kozikowski, A. P.; Mease, R. C.; Pomper, M. G.; Lubkowski, J. *J. Med. Chem.* **2008**, *51*, 7737–7743.
(31) Banerjee, S. R.; Foss, C. A.; Castanares, M.; Mease, R. C.; Byun, Y.; Fox, J. J.; Hilton, J.; Lupold, S. E.; Kozikowski, A. P.; Pomper, M. G. *J. Med. Chem.* **2008**, *51*, 4504–4517.
(32) Banerjee, S. R.; Pullambhatla, M.; Byun, Y.; Nimmagadda, S.; Green, G.; Fox, J. J.; Horti, A.; Mease, R. C.; Pomper, M. G. *J. Med. Chem.* **2010**, *53*, 5333–5341.
(33) Zhang, A. X.; Murelli, R. P.; Barinka, C.; Michel, J.; Cocleaza, A.; Jorgensen, W. L.; Lubkowski, J.; Spiegel, D. A. *J. Am. Chem. Soc.* **2010**, *132*, 12711-12716.
(34) Douglas, T. H.; Morgan, T. O.; McLeod, D. G.; Moul, J. W.; Murphy, G. P.; Barren, R.; Sesterhenn, I. A.; Mostofi, F. K. *Cancer*, **1997**, *80*, 107-114.
(35) Xiao, Z.; Adam, B. L.; Cazares, L. H.; Clements, M. A.; Davis, J. W.; Schellhammer, P. F.; Dalmasso, E. A.; Wright, G. L. *Cancer Res.* **2001**, *61*, 6029 – 6033.
(36) Sokoloff, R. L.; Norton, K. C.; Gasior, C. L.; Marker, K. M.; Grauer, L. S. *The Prostate*, **2000**, *43*, 150–157.
(37) Tang, C. K.; Vaze, A.; Shen, M.; Rusling, J. F. *ACS Sens.* **2016**, *1*, 1036−1043.
(38) Su, S. L.; Huang, I. P.; Fair, W. R.; Powell, C. T.; Hesto, W. D. *Cancer Res.* **1995**, *55*, 1441-1443.
(39) Grauer, L. S.; Lawler, K. D.; Marignac, J. L.; Kumar, A.; Goel, A. S.; Wolfert, R. L. *Cancer Res.* **1998**, *58*, 4787-4789.
(40) Schmittgen, T. D.; Teske, S.; Vessella, R. L.; True, L. D.; Zakrajsek, B. A. *Int. J. Cancer*, **2003**, *107*,323–329.
(41) Cao, K. Y.; Mao, X. P.; Wang, D. H.; Xu, L.; Yuan, G. Q.; Dai, S. Q.; Zheng, B. J.; Qiu, S. P. *The Prostate*, **2007**, *67*, 1791-1800.
(42) Humphrey, P. A. *Modern Pathol.* **2004**, *17*, 292–306.
(43) Danila, D. C.; Fleisher, M.; Scher, H. I. *Clin. Cancer Res.* **2011**, *17*, 3903-3912.
(44) Nagrath, S.; Sequist, L. V.; Maheswaran, S.; Bell, D. W.; Irimia, D.; Ulkus, L.; Smith, M. R.; Kwak, E. L.; Digumarthy, S.; Muzikansky, A.; Ryan, P.; Balis, U. J.; Tompkins, R. G.; Haber, D. A.; Toner, M. *Nature,* **2007**, *450*, 1235-124.
(45) Giuliano, M.; Giordano, A.; Jackson, S.; Giorgi, U. D.; Mego, M.; Cohen, E. N.; Gao, H.; Anfossi, S.; Handy, B. C.; Ueno, N. T.; Alvarez, R. H.; Placido, S. D.; Valero, V.; Hortobagyi, G. N.; Reuben, J. M.; Cristofanilli, M. *Breast Cancer Res.* **2014**, *16*, 440-448.
(46) Joosse, S. A.; Gorges, T. M.; Pantel, K. *EMBO Mol. Med.* **2015**, *7*, 1-11.

Figure captions

Figure 1. Structure of PSMA-targeting DUPA*aFFC*-AMF-DOTA-Nd tag. The antenna moiety AMF absorbs exciting light (494 nm), and then transfer the energy to DOTA-Nd, emitting NIR light (841 nm, 1065 nm and 1350 nm). In addition, the core Nd can be accurately quantified using ICPMS to obtain the mass spectrometric signals with its isotopic distribution of ^{142}Nd (27.2 %), ^{143}Nd (12.2 %), ^{144}Nd (23.8 %), ^{145}Nd (8.3 %), ^{146}Nd (17.2 %), ^{148}Nd (5.7 %) and ^{150}Nd (5.6 %). Peptidomemitic DUPA*aFFC* can specifically target PSMA.

Figure 2. Emission spectra of $Nd(NO_3)_3$ (green line), AMF (black line), DUPA*aFFC*-AMF-DOTA (blue line), DUPA*aFFC*-AMF-DOTA-Nd (red line) of 10.0 μM each in 20 mM PBS buffer (pH 7.4). Two-step scanning from 450 nm to 800 nm (visible region) and then 800 nm to 1500 nm (NIR region) was performed under the excitation of 494 nm.

Figure 3. ICPMS and NIR responses from a series of $Nd(NO_3)_3$ (black solid square for ICPMS, red solid circle for NIR) and DUPA*aFFC*-AMF-DOTA-Nd (black open square for ICPMS, red open circle for NIR) solutions (0 - 250 nM), respectively.

Figure 4. SEC-ICPMS chromatograms of DUPA*aFFC*-AMF-DOTA-Nd (15 nM) (black line) and, the mixture of PSMA (5 nM) with DUPA*aFFC*-AMF-DOTA-Nd (15 nM) (red line). ^{142}Nd was monitored; a Superdex 75 10/300 GL column (10 mm I.D. × 300 mm in length) and 50 mM ammonium bicarbonate (pH 7.4) mobile phase with the flow rate of 0.8 mL/min were used.

Figure 5. Relationship between the LNCaP cell number and the intensity of ICPMS (black square) or NIR (red circle). Log 10 scale was used after the break (x axis break from 1 to 100, Y axis for ICPMS from 0.01 to 0.1, for NIR from 1 to 100) at 5% of the axis.

Figure 6. Boxplots of *t*PSMA concentrations in the PCa with different Gleason score, BPH, healthy male and female blood samples. The boxes represent the 25th and 75th percentiles; the whiskers represent the 5th and 95th percentiles; and outliers are displayed by circles. The black lines represent the median value; the red lines represent the mean value

For TOC only

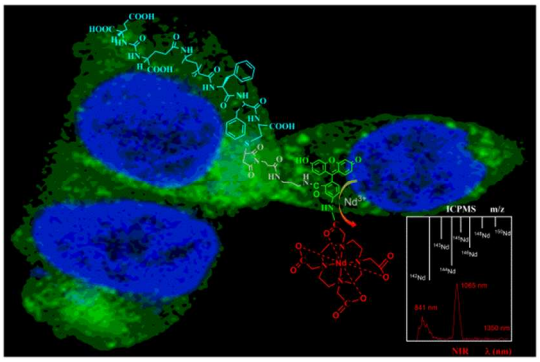
COOH
HOOC
Nd3+
ICPMS m/z
NIR λ (nm)